Proceedings of the ASME 2010 3rd Joint US-European Fluids Engineering Summer Meeting and 8th International Conference on Nanochannels, Microchannels, and Minichannels
FEDSM-ICNMM2010
August 1-5, 2010, Montreal, Canada

FEDSM-ICNMM2010-30167

GAS MICROFLOWS IN THE SLIP FLOW REGIME: A REVIEW ON HEAT TRANSFER

Stéphane Colin
Université de Toulouse; INSA, UPS, Mines Albi, ISAE; ICA (Institut Clément Ader)
135 avenue de Rangueil, F-31077 Toulouse, France

ABSTRACT

Accurate modeling of gas microvection is crucial for a lot of MEMS applications (micro-heat exchangers, pressure gauges, fluidic microactuators for active control of aerodynamic flows, mass flow and temperature micro-sensors, micropumps and microsystems for mixing or separation for local gas analysis, mass spectrometers, vacuum and dosing valves…). Gas flows in microsystems are often in the slip flow regime, characterized by a moderate rarefaction with a Knudsen number of the order of 10^{-2} - 10^{-1}. In this regime, velocity slip and temperature jump at the walls play a major role in heat transfer.

This paper presents a state of the art review on convective heat transfer in microchannels, focusing on rarefaction effects in the slip flow regime. Analytical and numerical models are compared for various microchannel geometries and heat transfer conditions (constant heat flux or constant wall temperature). The validity of simplifying assumptions is detailed and the role played by the kind of velocity slip and temperature jump boundary conditions is shown. The influence of specific effects, such as viscous dissipation, axial conduction and variable fluid properties is also discussed.

1. INTRODUCTION

Due to the trend of miniaturization of electromechanical systems, there is an increasing need for micro heat exchangers. The applications concern for example the cooling of electronic components, MEMS or MOEMS. More generally, heat transfer is involved in most of microfluidic systems, and especially in those that use gases. In addition to compressibility, rarefaction of the flow at small scale has a significant impact on heat transfer.

In fluidic microsystems, shrinking down the dimensions leads to an increase of the Knudsen number:

$$Kn = \frac{\lambda}{D_h} \tag{1}$$

defined as the ratio of the mean free path λ of the molecules other a characteristic length, for example the hydraulic diameter D_h of a microchannel. The Knudsen number encountered in classic microsystems is frequently between 10^{-3} and 10^{-1}, which is the typical range of the well-known slip flow regime [1]. In this moderate rarefied regime, velocity slip and temperature jump at the wall strongly influences heat transfer. In the past ten years, a number of theoretical and numerical studies have been aimed at modeling gas convective heat transfer in microchannels, taking into account rarefaction effects.

Reviews on this topic are dating, do not focus on gases and do not take into account the last research contributions. Sobhan and Garimella [2] presented in 2001 a compilation and analysis of the results from investigations on fluid flow and heat transfer in micro- and mini-channels, with special emphasis to experimental studies. The case of both liquids and gases was treated, but without analysis of rarefaction effects on gas microconvection. In 2001, Rostami et al. [3] published a review devoted to gaseous flows in microchannels, but the analysis was essentially focused on hydrodynamics and not on heat transfer. More recently, in 2004, Morini [4] reviewed experimental studies on single-phase convective heat transfer in microchannels. Most of the papers listed in this review concerned heat transfer with liquids; only four studies were including data on Nusselt numbers for gases in microchannels. Moreover, the dimensions were such that rarefaction effects were negligible.

The objective of this paper is to present a detailed review of investigations on slip flow heat transfer in microchannels. The analysis is focused on the Nusselt number, and its dependence vis-à-vis rarefaction effects (Knudsen number), viscous dissipation effects (Brinkman number) and axial conduction effects (Peclet number).

NOMENCLATURE

a	fraction of the surface covered by adsorbed atoms, Langmuir's model
b	half-width of rectangular section or minimal half-width of trapezoidal section
Br	Brinkman number, dimensionless
Br_{φ}	modified Brinkman number, dimensionless
c_p	specific heat capacity at constant pressure, J kg^{-1} K^{-1}
D_h	hydraulic diameter, m
h	half-depth of parallel plate channel or of rectangular section; depth of trapezoidal section
k	thermal conductivity, W m^{-1} K^{-1}
Kn	Knudsen number, dimensionless
n	normal coordinate, m
Nu	Nusselt number, dimensionless
p	pressure, Pa
Pe	Peclet number, dimensionless
Pr	Prandtl number, dimensionless
r_0	radius of circular section, m
R	specific gas constant, J kg^{-1} K^{-1}
t	streamwise coordinate, m
T	temperature, K
u	streamwise velocity, m s^{-1}
v	normal velocity, m s^{-1}

Greek symbols

φ	heat flux, W m^{-2}
ϕ	angle of trapezoidal section, rad
γ	ratio of specific heats, dimensionless
λ	mean free path, m
μ	dynamic viscosity, Pa s
ρ	density, kg m^{-3}
σ_T	thermal accommodation coefficient, dimensionless
σ_u	tangential momentum accommodation coefficient, dimensionless
ξ^*	coefficient of slip, dimensionless
ς^*	temperature jump distance, dimensionless

Subscripts

w	at the wall
∞	fully developed conditions

Acronyms

AE	analytical model - explicit formulation
AI	analytical model - implicit formulation
C	circular microtube
CHF	constant heat flux
CWT	constant wall temperature
E	experimental study
HFDF	hydrodynamically fully developed flow
N	numerical simulation
PP	parallel plate microchannel
TFDF	thermally fully developed flow
TDF	thermally developing flow
TR	trapezoidal microchannel
UHW	unsymmetrically heated walls
1WI	one wall insulated
2WI	two walls insulated

2. SCOPE OF THE REVIEW

In this review, we consider pressure driven flows of gases with heat transfer in straight microchannels with constant cross-section (see Fig. 1). Heat transfer in circular microchannels is analyzed in section 4, the case of parallel plate microchannels is discussed in section 5, rectangular and trapezoidal or triangular sections are considered in sections 6 and 7 respectively, whereas other sections are treated in section 8.

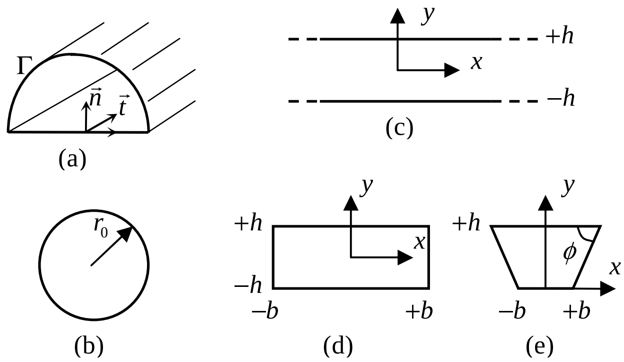

FIGURE 1: DIFFERENT CROSS SECTIONS OF MICROCHANNELS CONSIDERED IN THIS REVIEW.

The flow is laminar and the regime is the slip flow regime. Investigations on thermally fully developed and thermally developing flows (TFDF and TDF), with constant heat flux (CHF) or constant wall temperature (CWT) are reviewed. The different slip flow and temperature jump boundary conditions are presented in section 3.

3. SLIP FLOW AND TEMPERATURE JUMP BOUNDARY CONDITIONS

From a theoretical point of view, the slip flow regime is particularly interesting because it generally leads to analytical or semi-analytical models. In this regime, continuum Navier-Stokes equations are still valid, provided they are associated with velocity-slip and temperature-jump boundary conditions. Different forms of these boundary conditions can be found in the literature; the most frequently used and relevant for this review are listed below.

Velocity slip boundary conditions

First-order slip boundary conditions have been first written by Maxwell, and can be found on different simplified forms in the literature. The simplest one does not take into account thermal creep and assumes a totally diffuse reflection at the wall:

$$u - u_w = \lambda \left. \frac{\partial u}{\partial n} \right|_\Gamma . \quad (2)$$

Although the tangential momentum accommodation coefficient σ_u is generally found to be close to unity [5], lower values can be considered using the boundary condition

$$u - u_w = \frac{2-\sigma_u}{\sigma_u} \lambda \left. \frac{\partial u}{\partial n} \right|_\Gamma \quad (3)$$

and thermal creep effects due to an axial temperature gradient are considered in:

$$u - u_w = \frac{2-\sigma_u}{\sigma_u} \lambda \left. \frac{\partial u}{\partial n} \right|_\Gamma + \frac{3}{4} \frac{\mu R}{p} \left. \frac{\partial T}{\partial t} \right|_\Gamma . \quad (4)$$

In some cases, the previous equation is extended as (in somes papers, the term du/dt is written dv/dt):

$$u - u_w = \frac{2-\sigma_u}{\sigma_u} \lambda \left. \left(\frac{\partial u}{\partial n} + \frac{\partial u}{\partial t} \right) \right|_\Gamma + \frac{3}{4} \frac{\mu R}{p} \left. \frac{\partial T}{\partial t} \right|_\Gamma . \quad (5)$$

The second term of the RHS is often neglected in theoretical analysis, as it is of $\vartheta\left(Kn^2\right)$, while the first term is $\vartheta\left(Kn\right)$. The accuracy of the first term could be improved, adding a correcting coefficient –of the order of 1.1– calculated from the kinetic theory. Including the actual value of σ_u, first-order slip boundary condition can be written in a more general form as:

$$u - u_w = \beta_{u1} \lambda \left. \frac{\partial u}{\partial n} \right|_\Gamma \quad (6)$$

with β_{u1} is generally slightly higher than unity. Second-order boundary conditions have been proposed in the literature, in an attempt to increase the Knudsen range of applicability of the slip flow regime. In the specific case of a plane flow, they can be written on the general form [6]:

$$u - u_w = \beta_{u1} \lambda \left. \frac{\partial u}{\partial n} \right|_\Gamma + \beta_{u2} \lambda^2 \left. \frac{\partial^2 u}{\partial n^2} \right|_\Gamma \quad (7)$$

with different values proposed in the literature for β_{u2}. Another kind of slip boundary condition is the one of Langmuir's model, which takes into account adsorption/desorption of gas molecules at the wall and reads:

$$u = a\, u_w + (1-a)\, u_{(n=\lambda)} \quad (8)$$

where a is the fraction of the surface covered by adsorbed atoms.

In the same way, temperature jump boundary conditions are proposed in different first-order or second-order forms:

$$T - T_w = \frac{2\gamma}{\gamma+1} \frac{\lambda}{Pr} \left. \frac{\partial T}{\partial n} \right|_\Gamma \quad (9)$$

$$T - T_w = \frac{2-\sigma_T}{\sigma_T} \frac{2\gamma}{\gamma+1} \frac{\lambda}{Pr} \left. \frac{\partial T}{\partial n} \right|_\Gamma \quad (10)$$

$$T - T_w = \beta_{T1} \lambda \left. \frac{\partial T}{\partial n} \right|_\Gamma \quad (11)$$

$$T - T_w = \beta_{T1} \lambda \left. \frac{\partial T}{\partial n} \right|_\Gamma + \beta_{T2} \lambda^2 \left. \frac{\partial^2 T}{\partial n^2} \right|_\Gamma \quad (12)$$

$$T = a\, T_w + (1-a)\, T_{(n=\lambda)} \quad (13)$$

Equations (9), (10), (11), (12) and (13) are generally used in parallel with eqs. (2), (3), (6), (7) and (8), respectively.

4. HEAT TRANSFER IN CIRCULAR MICROCHANNELS

Heat transfer in circular microtubes has been extensively studied, both analytically and numerically, for gas flows in the slip flow regime (see Table 1). We consider in this section a microchannel with circular cross section, the radius of which is r_0 (see Fig. 1b).

4.1. Fully developed flow and uniform wall heat flux

The problem of hydrodynamically and thermally fully developed flow (HFDF and TFDF, respectively) in a microtube with uniform and constant heat flux (CHF) at the wall has been analytically solved in the slip flow regime by Sparrow and Lin [7]. They used classic first-order boundary conditions (3)-(10) and obtained an exact expression for the Nusselt number, which can be written as:

$$Nu_{(\mathrm{C},\infty,\mathrm{CHF})} = \left(\frac{\varsigma_r *}{2} + \frac{11 + 64\xi_r * + 96\xi_r *^2}{48\left(1+4\xi_r *\right)^2} \right)^{-1} . \quad (14)$$

In this equation,

$$\xi_r * = \frac{2-\sigma_u}{\sigma_u} \frac{\lambda}{r_0} \quad (15)$$

is the dimensionless coefficient of slip and

$$\varsigma_r * = \frac{2-\sigma_T}{\sigma_T} \frac{2\gamma}{\gamma+1} \frac{1}{Pr} \frac{\lambda}{r_0} \quad (16)$$

is the dimensionless temperature jump distance.

In the absence of rarefaction effects, both coefficients $\xi_r *$ and $\varsigma_r *$ are zero and the Nusselt number has the classic value $48/11 = 4.36$. We can extend the validity of Eq. (14) to more general first-order boundary conditions such as (6) and (11), provided the definition of the coefficient of slip and the temperature jump distance are generalized as $\xi_r * = \beta_{u1}\lambda/r_0$ and $\varsigma_r * = \beta_{T1}\lambda/r_0$, respectively. The Nusselt number can then be expressed as a function of the Knudsen number

$$Kn = \frac{\lambda}{2 r_0} \tag{17}$$

as:

$$Nu_{(\mathrm{C},\infty,\mathrm{CHF})} = \left(\beta_{T1} Kn + \frac{11 + 128 \beta_{u1} Kn + 384 \beta_{u1}^2 Kn^2}{48 \left(1 + 8 \beta_{u1} Kn\right)^2} \right)^{-1} . \tag{18}$$

TABLE 1: SUMMARY OF INVESTIGATIONS ON SLIP FLOW HEAT TRANSFER IN MICROTUBES.

Refs. Year	Kind of Work	Heat Conditions	Assumptions Particular Effects taken into account	BC
[7] 1962	AE	CHF	HFDF, TFDF	(3)-(10)
			+ thermal creep	(4)-(10)
	AI	CWT	HFDF, TFDF	(3)-(10)
[8] 1997	AE	CHF	HFDF, TFDF	(2)-(9)
	AI		HFDF, TDF	
[9] 2000	AE	CHF	HFDF, TFDF, variable *μ* and *k* near the wall	no *u*-slip, no *T*-jump
[10] 2001	AI	CHF CWT	HFDF, TDF, viscous heating	(2)-(9)
[11] 2006	AE	CHF CWT	HFDF, TFDF, viscous heating	(2)-(9)
[12] 2006	A	CHF CWT	HFDF, TDF, viscous heating, axial conduction	(3)-(10)
[13] 2007	AE	CHF CWT	HFDF, TFDF, viscous heating	(2)-(9)
[14] 2010	AI	CHF	HFDF, TFDF, viscous heating, $\mu(T)$, $k(T)$	(3)-(10)
[15] 2009	AE	CWT	HFDF, TFDF, viscous heating, $\mu(T)$, $k(T)$	(3)-(10)
[16-18] 1996-97	AI	CWT	HFDF, TDF	(2) no *T*-jump
[19] 2000	A	CWT	HFDF, TDF	(6)-(11)
[20] 2006	A	CWT	HFDF, TDF axial conduction	(8)-(13)
[21] 2009	AI	CHF	HFDF, TDF, viscous heating, axial conduction	(2)-(10)
[22] 2008	N	CWT	HFDF, TDF, viscous heating, axial conduction	(2)-(10)
[23] 2010	AI	CWT	HFDF, TDF, axial conduction	slug flow (9)
[24] 2009	E	Outer heating flow	Stainless steel tubes	

The same result has been demonstrated by Ameel et al. [8] in the case of full accommodation, with the boundary conditions (2) and (9), which correspond to $\beta_{T1} = 2\gamma / \left[(\gamma+1) Pr \right]$ and $\beta_{u1} = 1$. It is also possible to include thermal creep effects, replacing the boundary condition (3) with the boundary condition (4). Sparrow and Lin [7] showed that this leads to a correction of Eq. (14).

Equation (14) points out that the velocity slip tends to increase the Nusselt number, while the temperature jump decreases it. In most practical cases, the later effect is predominant, and the Nusselt number is reduced, as rarefaction increases.

Li et al. [9] studied the same problem of fully developed flow with constant heat flux at the wall. They kept classic boundary conditions, i.e. no velocity slip and no temperature jump, but they assumed a wall-adjacent layer in which the viscosity and thermal conductivity differ from those in the bulk flow. The thickness of this layer is about 3 to 5 times the mean free path of the molecules and the modification of viscosity and thermal conductivity in this layer is calculated from a simplified kinetic theory assuming hard sphere molecules and full accommodation ($\sigma_u = \sigma_T = 1$) at the wall. This analysis leads to:

$$Nu_{(\mathrm{C},\infty,\mathrm{CHF})} = \frac{48 \left(1 + 4.1075 Kn\right)^2}{11 \left(1 + 10.4556 Kn + 18.4057 Kn^2\right)} . \tag{19}$$

In this equation, the Nusselt number does not depend on the Prandtl number, neither on the ratio γ of the specific heats. Although Eq. (19) shows the same tendency as Eq. (18), it underestimates the decrease of the Nusselt number when rarefaction increases (see Fig. 2).

Effects of viscous heating

Effects of viscous heating have been taken into account by Tunk and Bayazitoglu [10] in 2001 and later by Aydın and Avcı [11] and Jeong and Jeong [12], both in 2006, then by Hooman [13] in 2007. They introduced the modified Brinkman number

$$Br_\varphi = \frac{\mu \bar{u}^2}{\varphi_w D_h} = \frac{\mu \bar{u}^2}{2 \varphi_w r_0} , \tag{20}$$

where $\bar{u}$ is the mean velocity and φ_w the uniform heat flux at the wall transmitted to the fluid. In [10, 11, 13], boundary conditions (2)-(9) were considered, i.e. full accommodation was assumed, whereas in [12], more general boundary conditions (3)-(10) were considered. Tunk and Bayazitoglu [10] solved the problem by the integral transform technique and provided calculated data for $Br_\varphi = 0.01$ and $Br_\varphi = -0.01$. Aydın and Avcı [11] obtained an analytical solution of the Nusselt number:

$$Nu_{(\mathrm{C},\infty,\mathrm{CHF},Br_\varphi \neq 0)} = \frac{8}{1 + \frac{2}{3C_1} + \frac{1 + 16 Br_\varphi}{6 C_1^2} + \frac{4 Br_\varphi}{C_1^3} + \frac{4 Br_\varphi}{3 C_1^4} + \frac{16 \gamma Kn}{(\gamma+1) Pr}} \tag{21}$$

where

$$C_1 = 1 + 8 Kn . \tag{22}$$

Equation (21) generalises Eq. (18), taking into account viscous dissipation, in the case $\beta_{u1} = 1$ and $\beta_{T1} = 2\gamma / [(\gamma+1)Pr]$. As for Jeong and Jeong [12], they found the solution:

$$Nu_{(C,\infty,CHF,Br_\varphi \neq 0)} = \frac{48 C_2^2}{C_2^2 \left(6C_2^2 + 4C_2 + 1 + 48 C_2^2 C_3\right) + 8 Br_\varphi \left(2C_2^2 + 3C_2 + 1\right)} \quad (23)$$

with

$$C_2 = 1 + 8\,Kn\left(2 - \sigma_v\right)/\sigma_v \quad (24)$$

and

$$C_3 = \left(2 - \sigma_T\right) 2\gamma Kn / \left(\sigma_T Pr\left(\gamma + 1\right)\right). \quad (25)$$

For a heated surface ($Br_\varphi > 0$), an increase of viscous heating leads to a decrease of the Nusselt number, whereas for a cooled surface ($Br_\varphi < 0$), the opposite is observed. The data provided by Tunk and Bayazitoglu are in rough agreement with Eqs. (21) and (23), although the effect of viscous dissipation they predicted is more pronounced for low Knudsen numbers, at least for $Br_\varphi = 0.01$ and $Br_\varphi = -0.01$ (see Fig. 2). Hooman [13] also proposed an analytical solution of $Nu(Kn, Pr, Br_\varphi)$, but there is in all likelihood a typo in the equations reported in his paper, which does not allow a precise comparison with the previous studies. The plotted results for $Br_\varphi = -0.01$, however, seems to be in close agreement with those calculated by Eqs. (21) and (23).

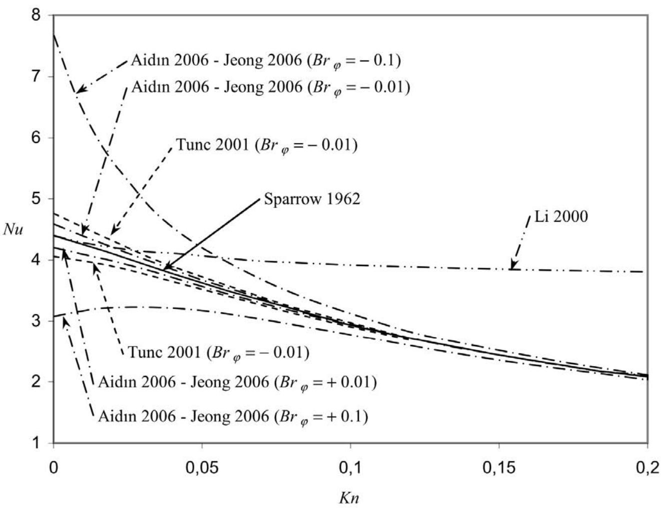

FIGURE 2: NUSSELT NUMBER FOR FULLY DEVELOPED FLOW IN A MICROTUBE WITH UNIFORM WALL HEAT FLUX AS A FUNCTION OF KNUDSEN NUMBER.

Effects of radial fluid properties variation

Hooman and Ejlali [14] recently extended their model, taking into account, in addition to viscous dissipation, the radial variation of the viscosity μ and the thermal conductivity k with the temperature. Their study is based on a perturbation technique, assuming

$$\mu = \mu_w \left(1 + \varepsilon\,\theta\right), \quad (26)$$

$$k = k_w \left(1 + \varepsilon_k\,\theta\right), \quad (27)$$

were ε and ε_k are small parameters and θ is the dimensionless temperature difference between the local temperature and the temperature in the fluid at the wall. The model is illustrated with data for $\varepsilon = \varepsilon_k = -0.2$, $Pr = 0.7$, $\gamma = 1.4$ and $\sigma_u = \sigma_T = 1$. The Nusselt number is increased, with a value close to 4.65 for the limit $Kn = Br_\varphi = 0$. It would be interesting to compare results from this model with numerical simulations performed by a CFD code.

A comparison of fully developed Nusselt number $Nu_{(C,\infty,CHF)} = fct(Kn)$ for CHF, calculated from the studies cited above, is shown in Fig. 2, in the case of a gas with a Prandtl number $Pr = 0.7$ and a specific heat ratio $\gamma = 1.4$, and for accommodation coefficients $\sigma_u = \sigma_T = 1$.

4.2. Fully developed flow and uniform wall temperature

TABLE 2: NUSSELT NUMBER FOR FULLY DEVELOPED FLOW IN A MICROTUBE WITH UNIFORM WALL TEMPERATURE, IN FUNCTION OF SLIP FLOW AND TEMPERATURE JUMP COEFFICIENTS. DATA DERIVED FROM SPARROW AND LIN [7].

$\xi_r^* = 0.04$		$\xi_r^* = 0.1$		$\xi_r^* = 0.2$		$\xi_r^* = 0.3$		$\xi_r^* = 0.5$	
ς_r^*	Nu_∞	ς_r^*	Nu_∞	ς_r^*	Nu_∞	ς_r^*	Nu_∞	ς_r^*	Nu_∞
.03698	3.6450	.1614	3.2131	.3212	2.7378	.4896	2.3113	.8188	1.7298
.06670	3.4880	.1665	3.1903	.3338	2.6953	.5016	2.2813	.8336	1.7085
.06732	3.4848	.1815	3.1250	.3492	2.6450	.6002	2.0605	1.035	1.4621
.08838	3.3800	.2114	3.0013	.4248	2.4200	.7308	1.8241	1.250	1.2664
.09974	3.3256	.2426	2.8800	.5002	2.2282	.7500	1.7936	1.315	1.2168
.1214	3.2258	.2496	2.8541	.5102	2.2050	.8870	1.6021	1.500	1.0952
.1444	3.1250	.3106	2.6450	.6076	2.0000	1.077	1.3945	1.687	.99405
.1556	3.0777	.3474	2.5313	.7198	1.8050	1.165	1.3146	1.938	.88445
.1743	3.0013	.3866	2.4200	.7790	1.7161	1.311	1.2013	1.945	.88179
.2058	2.8800	.3890	2.4134	.8088	1.6745	1.449	1.1101	2.1978	.79380
.2390	2.7613	.4724	2.2050	.9546	1.4965	1.605	1.0225	2.5042	.70805
.2668	2.6681	.5196	2.1013	1.090	1.3613	1.798	.93161	2.9274	.61605
.2740	2.6450	.5806	1.9801	1.225	1.2482	1.983	.85805	3.3100	.55125
.2922	2.5878	.6356	1.8818	1.333	1.1705	1.999	.85217	3.3274	.54863
.3110	2.5313	.6676	1.8288	1.3354	1.1689	2.094	.81920	3.6826	.50000

Sparrow and Lin [7] studied the case of fully developed flow with uniform and constant wall temperature (CWT). The eingenvalue problem was numerically solved, and the derived Nusselt number is provided in Table 2 as a function of coefficients ξ_r* and ς_r*. When $\xi_r* \to 0$ and $\varsigma_r* \to 0$, the Nusselt number tends to the classic value 3.66.

Baron et al. [16, 17] and Mikhailov and Cotta [18] studied the same problem, but they did not take into account temperature jump at the wall. As a consequence, they found that the Nusselt number increases with the Knudsen number, due to the slip of velocity (see Fig. 3). As the temperature jump, however, plays the main role in practical cases, a decrease of Nusselt number is expected when rarefaction increases, as predicted by Sparrow and Lin.

Effects of viscous heating

The effect of viscous heating has been taken into account by Tunc and Bayatoziglu [10], Aydın and Avcı [11], Jeong and Jeong [12] and Hooman [13]. The intensity of viscous dissipation is quantified by the Brinkman number

$$Br = \frac{\mu \bar{u}^2}{k\left(T_0 - T_w\right)}, \tag{28}$$

where T_0 is the temperature of the fluid at the tube entrance and k its thermal conductivity. In the case of CHF, the fully developed Knudsen number depends on the value of the modified Brinkman number. Conversely, in the CWT case, when viscous dissipation is taken into account, whatever the Brinkman number, the fully developed Nusselt number is only function of the Knudsen number [12]. Moreover, it can be explicitly obtained, while for $Br = 0$, the implicit solution requires a numerical calculation. Jeong and Jeong [12] obtained:

$$Nu_{(\mathrm{C},\infty,\mathrm{CWT},Br\neq 0)} = \frac{48C_1}{1+4C_1+48C_1C_2}, \tag{29}$$

Hooman [13] found the same result in the case of full accommodation, for $\sigma_u = \sigma_T = 1$. For $Kn = 0$, the solution tends to $48/5 = 9.6$. Values obtained for $Kn = [0; 0.04; 0.08]$ are confirmed by Çetin et al. [22]. On the other hand, Tunc and Bayatoziglu [10] found a limit value of 6.42, lower than the expected one (see Fig. 3).

Effects of radial fluid properties variation

As in the CHF case, Hooman et al. [15] took into account the radial variation of viscosity and thermal conductivity with the temperature, according to Eqs. (26) and (27). They obtained an explicit expression of the Nusselt number. For $\varepsilon = \varepsilon_k = 0.2$, $Pr = 0.7$, $\gamma = 1.4$ and $\sigma_u = \sigma_T = 1$, it is observed that the effect of properties variation on the Nusselt number is negligible.

A comparison of the values of fully developed Nusselt number $Nu_{(\mathrm{C},\infty,\mathrm{CWT})} = fct(Kn)$ calculated from the studies cited above is shown in Fig. 3, in the case of a gas with a Prandtl number $Pr = 0.7$ and a specific heat ratio $\gamma = 1.4$, and for accommodation coefficients $\sigma_u = \sigma_T = 1$.

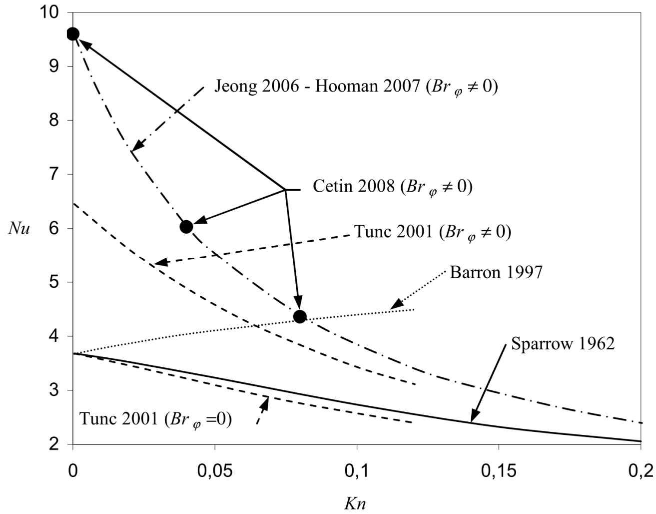

FIGURE 3: NUSSELT NUMBER FOR FULLY DEVELOPED FLOW IN A MICROTUBE WITH UNIFORM WALL TEMPERATURE AS A FUNCTION OF KNUDSEN NUMBER.

4.3. Developing flow: the extended Graetz problem

The problem of developing flow has been studied by several authors. It is an extension to the slip regime of the Graetz problem, which considers a hydrodynamically fully developed flow and a thermally developing flow (TDF), the gas experiencing heat transfer at the entrance of the microtube due to a constant heat flux or a constant temperature imposed at the wall. In the Graetz problem, the flow is assumed steady and incompressible, with constant fluid properties, no swirl component of velocity and negligible dissipation effects. Moreover, an implicit assumption is that of a high Peclet number *Pe*, which means that the axial conduction is negligible in comparison with the axial convection. Several authors have extended the analysis of Graetz, who initially assumed $Kn = 0$, $Br = 0$ and $Pe \to \infty$, by taking into account rarefaction ($Kn \neq 0$) and in some cases including viscous dissipation ($Br \neq 0$) and axial conduction (finite *Pe*) effects.

Constant heat flux

Ameel et al. [8] calculated the velocity profile and the Nusselt number in the entrance region of a microtube for a thermally developing flow with a uniform temperature T_0 at the entrance ($z = 0$) and a constant heat flux at the wall for $z > 0$. They obtained an extension of Eq. (18) for total accommodation at the wall. The thermal entrance length z_e, defined as the heated length required for the Nusselt number to approach within 5 % of the fully developed value, was found to increase with the Knudsen number. On a dimensionless form, $z_e^+ = z_e / (r_0 \, Re \, Pr)$ was fitted by a polynomial as:

$$z_e^+ = 0.0828 + 0.5030\,Kn - 3.0804\,Kn^2 + 8.6806\,Kn^3 \quad (30)$$

Calculation was made for a gas with a Prandtl number $Pr = 0.7$ and a heat ratio $\gamma = 1.4$.

Effects of viscous dissipation and of axial conduction have been taken into account by Jeong and Jeong [12] and by Çetin et al. [21]. Coupled effects of *Kn*, *Pe* and Br_φ on *Nu* are discussed in [21]. Data found in the fully developed region are in close agreement with those from [11, 12]. The thermal entrance length increases as Pe decreases, due to the increased effect of axial conduction. Increasing the Brinkman number leads to a decrease of the Nusselt number, and the influence of viscous dissipation is less pronounced as rarefaction increases, which confirms what is observed in the fully developed region.

Constant wall temperature

A first analysis of the Graetz problem with constant temperature at the wall can be found in [7], although the goal of the study from Sparrow and Lin was to determine the fully-developed Nusselt number value, obtained far from the entrance region. Data on Nusselt numbers in the entrance region were provided for the specific case $Pr = 0.7$, $\gamma = 1.4$ and $\sigma_u = \sigma_T = 1$. The same problem was more recently treated by Barron et al. [16, 17], who experienced numerical instabilities issues fixed later by Mikhailov and Cotta [18]. In these papers, however, the authors did not take into account the temperature jump at the wall although they cited the boundary condition (10). As a consequence, they neglected the main contribution of rarefaction effects on the heat transfer and found an increase in the Nusselt number as the Knudsen number was increased. This is illustrated in Fig. 3, which shows the fully-developed Nusselt number corresponding to TFDF calculated in [16, 17]. This issue was later fixed by Larrodé et al. [19], who used the first-order boundary conditions (6) and (11). Their results were presented in function of $\beta = \beta_{T1}/\beta_{u1}$ and they were in agreement with those from Barron et al. in the limit case where $\beta = 0$, when the temperature jump is neglected. For a gas with a Prandtl number $Pr = 0.7$ and a heat ratio $\gamma = 1.4$ and full accommodation at the wall, however, $\beta = 1.67 > 1$ and heat transfer decreases as rarefaction increases.

The effects of viscous dissipation were treated by Tunc and Bayazitoglu [10]. Although the fully developed Nusselt number does not depend on the value of the Brinkman number *Br*, in the thermally developing region, an increase of *Br* leads to an increase of *Nu*. The values provided in [10] should be considered with precaution, however, as the values calculated in the fully developed region differ from those calculated in [13].

A more detailed analysis can be found in [22], in which axial conduction is also considered. Taking into account axial conduction complicates the problem due to the presence of the non self-adjoint eingenvalue problem, which makes the linearly independent eingenfunctions non-orthogonal. Çetin et al. [22] solved the energy equation numerically by using finite difference scheme. They observed that for $Br = 0$ the local Nusselt number Nu increases with decreasing Pe, as it is the case for Nu_∞. The thermal entrance length also increases with decreasing Pe. For $Br > 0$, corresponding to a cooling of the fluid, Nu experiences a jump due to viscous dissipation, the location of which depends on both Pe and Br. The fully developed value Nu_∞, however, is only function of Kn. For negative values of the Brinkman number, corresponding to a heating of the fluid, there exists a singular point where Nu goes to the infinity, because the bulk mean temperature of the fluid becomes equal to the wall temperature. Beyond this location, the fluid heats the wall.

The Graetz problem with CWT has also recently been studied by Myong et al. [20], who employed Langmuir boundary conditions (8) and (13), and compared the results with those obtained from the classic Maxwell boundary conditions (3) and (10). They found very similar trends, but a slightly more pronounced reduction of the Nusselt number due to rarefaction was observed. As an example, for a Knudsen number $Kn = 0.02$ and a monatomic gas, the reduction for the fully-developed Nusselt number was 5.7% with Maxwell boundary conditions and 8.3 % with the Langmuir model. In addition, the authors investigated the influence of the axial heat conduction. For $Pe = 10$, a significant increase of the Nusselt number is observed in the entrance region, and this effect decreases with increasing rarefaction.

In a recent paper, Satapathy [23] analyzed heat transfer for a thermally developing flow in a microtube with constant wall temperature, assuming uniform fluid velocity (slug flow) and taking into account axial conduction. The temperature boundary conditions were those of Eq. (10). There was no discussion, however, on how a slug flow of gas can be observed in a microtube, which limits the practical interest of this study.

4.4. Experimental data

There are very few experimental papers dealing with heat transfer with gases in circular microtubes, especially due to the difficulty to control thermal boundary conditions and to access local temperature measurements. Choi et al. [25] published experimental heat transfer data for a flow of nitrogen in microtubes with diameter of 9.7, 53 and 81.2 µm. The gas was heated at a temperature on the order of 60°C before entering the microtube and cooling was due to the lower temperature – approximately 20°C– of the air around the microtube. Thermocouples were mounted at 6 locations along the microtube to determine the bulk temperature distribution. In the laminar regime, a correlation was proposed for the fully developed Nusselt number depending both on the Prandtl and the Reynolds numbers. As the cooling conditions were not precisely controlled, it is difficult to draw sound conclusions on heat transfer from these experiments. Moreover, the inlet pressure was high (between 5.7 and 10 MPa) leading to negligible rarefaction effects with Knudsen numbers lower than 10^{-3}.

In a more recent study, Demsis et al. [24] provided first data on heat transfer with nitrogen in the slip flow regime. They investigated a range of the Knudsen number from 1.1×10^{-4} to 1.5×10^{-2}, using low pressures instead of low hydraulic diameters. The tube was a stainless steel tube with an inner diameter of 25 mm. It was heated by an outer flow of hot water. It was observed that the mean Nusselt number, based on a log mean temperature difference, decreased as *Kn* increased, which was expected from physical considerations. Very low values down to 6.2×10^{-4}, however, were measured in the slip flow regime.

5. HEAT TRANSFER IN PARALLEL PLATE MICROCHANNELS

A number of theoretical works have been devoted to heat transfer between parallel plates in the slip flow regime (see Table 3). In this section, the Knudsen number *Kn*, as well as the modified Brinkman number Br_φ, are still based on the hydraulic diameter, which is $D_h = 4h$ for parallel plates $2h$ away from each other (see Fig. 1c). Consequently, Eqs. (17) and (20) still hold, provided $D_h = 2r_0$ is replaced with $D_h = 4h$.

5.1. Fully developed flow and uniform wall heat flux

Inman [26] calculated the analytical solution of heat transfer for a HFDF and TFDF between parallel plates with one insulated wall (1IW) and an upper heated wall with uniform heat flux. The boundary conditions were first-order velocity slip (3) and temperature jump (10) conditions. They obtained the temperature profile and the Nusselt number:

$$Nu_{(\text{PP},\infty,\text{CHF-1WI})} = \left(\frac{\varsigma_h *}{4} + \frac{26+147\xi_h *+210\xi_h *^2}{140\left(1+3\xi_h *\right)^2} \right)^{-1}, \quad (31)$$

which reduces to the classic value $70/13 = 5.38$ when the Knudsen number is 0. In this equation,

$$\xi_h * = \frac{2-\sigma_u}{\sigma_u}\frac{\lambda}{h} = 4Kn\frac{2-\sigma_u}{\sigma_u} \quad (32)$$

is the dimensionless coefficient of slip and

$$\varsigma_h * = \frac{2-\sigma_T}{\sigma_T}\frac{2\gamma}{\gamma+1}\frac{1}{Pr}\frac{\lambda}{h} = \frac{2-\sigma_T}{\sigma_T}\frac{8\gamma}{\gamma+1}\frac{1}{Pr}Kn\,. \quad (33)$$

For a symmetrically heated microchannel, the solution is

$$Nu_{(\text{PP},\infty,\text{CHF})} = \left(\frac{\varsigma_h *}{4} + \frac{17+84\xi_h *+105\xi_h *^2}{140\left(1+3\xi_h *\right)^2} \right)^{-1}, \quad (34)$$

with the no-slip limit solution $140/17 = 8.24$. Zhu et al. [27] extended the solution to the case of two unsymmetrically heated walls (UHW) by combining the solutions of two sub-problems similar to the above problem.

TABLE 3: SUMMARY OF INVESTIGATIONS ON SLIP FLOW HEAT TRANSFER IN PARALLEL PLATE MICROCHANNELS.

Refs. Year	Kind of Work	Heat Conditions	Assumptions	BC
[26] 1964	AE	CHF-1WI	HFDF, TFDF	(3)-(10)
[27] 2002	AE	CHF-UHW	HFDF, TFDF	(3)-(10)
[9] 2000	AE	CHF	HFDF, TFDF, variable μ and k near the wall	no *u*-slip, no *T*-jump
[28] 2006	A	CHF CWT	HFDF, TDF, viscous heating, axial conduction	(3)-(10)
[29] 2007	AE	CHF CWT	HFDF, TFDF, viscous heating	(2)-(9)
[30] 2007	AE	CHF CWT	HFDF, TFDF, viscous heating	(7)-(12)
[14] 2010	AI	CHF	HFDF, TFDF, viscous heating, $\mu(T)$, $k(T)$	(3)-(10)
[31] 2002	N, AI	CWT	HFDF, TFDF, axial conduction	(2)-(9)
[15] 2009	AE	CWT	HFDF, TFDF, viscous heating, $\mu(T)$, $k(T)$	(3)-(10)
[32] 1997	N	CHF CWT	HDF, TDF compressibility	(2)-(9)
[33] 2000	AI	CWT	HFDF, TDF, axial conduction	(3)-(10)
[34] 2005	AI	CWT	HFDF, TDF, axial conduction	(3)-(10)
[35] 2009	N	CWT	Roughness	(5)-(10)
[36] 2006	N	CWT	Roughness	(7)-(12)
[37] 2009	N	CWT	Roughness, compressibility, viscous dissipation	(7)-(12)

Li et al. [9] studied the same problem of fully developed flow with constant heat flux at the wall, assuming a wall-adjacent layer in which the viscosity and thermal conductivity differ from those in the bulk flow. They found for $\sigma_u = \sigma_T = 1$:

$$Nu_{(\text{PP},\infty,\text{CHF-1WI})} = \frac{70\left(1+6.1614\,Kn\right)^2}{13\left(1+14.3764\,Kn+51.1024\,Kn^2\right)}. \quad (35)$$

for the case of one insulated wall, and

$$Nu_{(\text{PP},\infty,\text{CHF})} = \frac{140\left(1+6.1614\,Kn\right)^2}{17\left(1+14.3764\,Kn+52.104\,Kn^2\right)}. \quad (36)$$

for a symmetrically heated microchannel. Although Eqs. (35) and (36) show the same tendency as Eqs. (31) and (34), respectively, they underestimate the decrease of the Nusselt number when rarefaction increases (see Fig. 4).

Effects of viscous heating

Effects of viscous heating have been treated by Jeong and Jeong [28], who obtained the following analytical expression of the fully developed Nusselt number:

$$Nu_{(\mathrm{PP},\infty,\mathrm{CHF},Br_\varphi\neq 0)} = \frac{420\,C_4^2}{C_4^2\left(35C_4^2+14C_4+2+420C_4^2C_3\right)+4Br_\varphi\left(42C_4^2+33C_4+6\right)} \quad (37)$$

with

$$C_4 = 1+12\,Kn\left(2-\sigma_v\right)/\sigma_v \quad (38)$$

As for Aydın and Avcı [29], they obtained in the case $\beta_{u1}=1$ and $\beta_{T1}=2\gamma/\left[(\gamma+1)Pr\right]$:

$$Nu_{(\mathrm{PP},\infty,\mathrm{CHF},Br_\varphi\neq 0)} = \frac{3}{\frac{1}{2}+\frac{1}{5C_5}+\frac{\left(1+84Br_\varphi\right)}{35C_5^2}+\frac{66Br_\varphi}{35C_5^3}+\frac{12Br_\varphi}{35C_5^4}+\frac{12\,\gamma Kn}{(\gamma+1)Pr}} \quad (39)$$

where

$$C_5 = 1+12\,Kn\,. \quad (40)$$

Nusselt numbers calculated from Eqs. (31), (34), (35), (36) and (37) are plotted in Fig. 4, for a gas with $Pr=0.7$ and $\gamma=1.4$, and for accommodation coefficients $\sigma_u=\sigma_T=1$. Van Rij et al. [30] extended the solution to second-order boundary conditions.

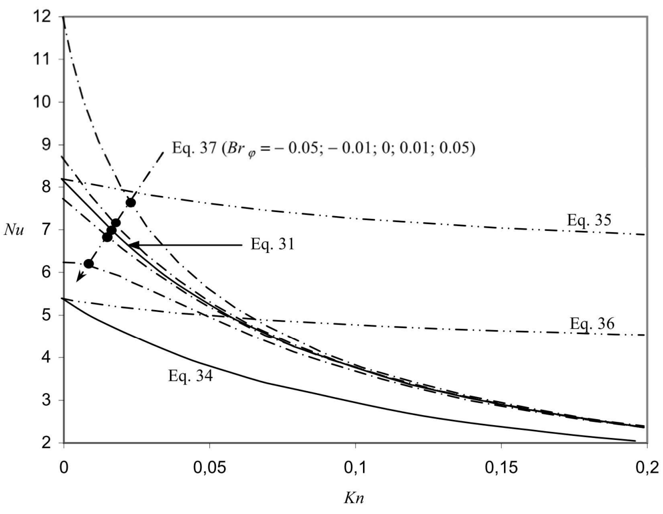

FIGURE 4: FULLY DEVELOPED NUSSELT NUMBER FOR A PARALLEL PLATE MICROCHANNEL FLOW WITH UNIFORM HEAT FLUX AS A FUNCTION OF KNUDSEN NUMBER.

Hooman and Ejlali [14] took into account, in addition, the radial variation of the viscosity μ and the thermal conductivity k with the temperature, through Eqs. (26) and (27). They drew similar conclusions as in the case of circular microtubes.

5.2. Fully developed flow and uniform wall temperature

The case of fully developed flow with uniform wall temperature was analyzed by Hadjiconstantinou and Simek [31], who took into account axial heat conduction. The boundary conditions were initially Eqs. (6)-(11), but the accommodation coefficients and correcting coefficients were absorbed in *Kn*, finally leading to the use of Eqs. (2)-(9). They compared the results from their analytical model with molecular simulations by the DSMC method, and found a good agreement between continuum and molecular results. They concluded that slip flow models, neglecting viscous dissipation, expansion cooling and thermal creep were able to capture heat transfer. The effect of axial heat conduction was to increase the Nusselt number.

Effects of viscous heating

In the CTW case, when viscous dissipation is taken into account, whatever the Brinkman number, the fully developed Nusselt number is only function of the Knudsen number [28]:

$$Nu_{(\mathrm{PP},\infty,\mathrm{CWT},Br\neq 0)} = \frac{140\,C_4}{1+7\,C_4+140\,C_4\,C_3}\,, \quad (41)$$

with a limit at 17.5 when $Kn\to 0$. Hooman [15] extended this solution, taking into account variable properties according to equations (26) and (27).

5.3. Extended Graetz problem

The extended Graetz problem was numerically studied by Kavehpour et al. [32] for both CWT and CHF conditions, using a control volume finite difference. They took into account compressibility effects and considered a thermally and hydrodynamically developing flow. They found that the Nusselt number was reduced taking into account rarefaction. Yu and Ameel [33] considered a thermally developing flow with constant wall temperature, taking into account axial conduction. According to the value of the ratio $\beta=\beta_{T1}/\beta_{u1}$, they found an increase or a decrease of heat transfer along the microchannel when rarefaction increases. A transition value of 0.2 separates the region of heat transfer enhancement from the region of heat transfer reduction. The value $\beta=1.67$, which correspond to a diffuse reflection $\sigma_u=1$) and a total thermal accommodation ($\sigma_T=1$) for air ($\gamma=1.4$; $Pr=0.7$) is a representative value, however, for many engineering applications. In this case, heat transfer is significantly reduced when the temperature jump is taken into account. Mikhailov and Cotta [34] analytically solved the same problem.

Jeong and Jeong [28] took in addition into account viscous dissipation, for both the CHF and CWT cases.

Roughness effects

Roughness effects have been taken into account by Khadem et al. [35], with slip boundary conditions adapted to curved surfaces in the CWT case. They also considered thermal creep in their numerical simulation. The wall roughness was modeled with periodically distributed triangular elements and random shaped micro peaks. It was found that roughness resulted in a decrease of Nusselt number and had more significant effect on higher Knudsen number flows with higher relative roughness. Ji et al. [36] considered the same problem with second-order boundary conditions and drew qualitative similar conclusions. Croce and d'Agaro [37] analyzed the competition between rarefaction and compressibility effects for high pressure drop flows in rough microchannels. They took into account viscous dissipation and covered a wide range of the Mach number. The slip boundary condition was (5) without the thermal creep term and with dv/dt in place of du/dt . It was found that compressibility was the most dominant effect at high Mach number, yielding even inversion of heat flux, while roughness had strong effects when rarefaction was significant.

6. HEAT TRANSFER IN RECTANGULAR MICROCHANNELS

Microchannels with rectangular cross-sections are frequently encountered in fluidic microsystems such as micro heat exchangers. There are easily manufactured, for example, by deep reactive ion etching in silicon wafers. Hydrodynamics of gases in such microchannels in the slip flow regime were analytically modeled, both with first-order [38] and second-order [39] boundary conditions. These models have been validated by experiments [5, 40]. The problem of heat transfer in rectangular microchannels is rather complicated because it requires 2D and 3D analysis and involves complex thermal boundary conditions, the most frequent of which are classified as [41, 42]:

i) Constant temperature at the wall (CWT);
ii) Uniform wall temperature along perimeter at a specified cross-section, with a linear evolution in the streamwise direction (H1);
iii) Constant wall heat flux (H2), with eight versions involving different combinations of heated and adiabatic walls: four heated sides (4), three heated sides and one adiabatic short side (3L), three heated sides and one adiabatic long side (3S), two heated long sides and two adiabatic short sides (2L), two heated short sides and two adiabatic long sides (2S), one short and one long heated sides (2C), one heated long side (1L) and one heated short side (1S).

In addition, the aspect ratio h/b of the cross section (see Fig. 1d) is another parameter to take into account. Table 4 gives a summary of recent investigations of heat transfer in rectangular microchannels in the slip flow regime.

TABLE 4: SUMMARY OF INVESTIGATIONS ON SLIP FLOW HEAT TRANSFER IN RECTANGULAR MICROCHANNELS.

Refs. Year	Kind of Work	Heat Conditions	Assumptions	BC
[43] 2001	AI	CWT	HFDF, TDF	(3)-(10)
[44] 2002	AI	H2-4	HFDF, TFDF	constant *u*-slip, (9)
[45] 2002	AI	H2-4	HFDF, TDF	(3)-(10)
[46] 2005	AI	H1	HFDF, TFDF	(3)-(10)
[47] 2006	N	CWT	HDF, TDF	(2)-(9)
[48] 2006	AI	H1	HFDF, TFDF, viscous heating	(3)-(10)
[49] 2007	AI	H2 (8 versions)	HFDF, TFDF	(3)-(10)
[50] 2008	N	CWT H2-4	HFDF, TDF, wall conduction, axial conduction	(2)-(9)
[51] 2008	N	CWT	HDF, TDF	(2)-(9)
[52] 2008	N	H1	HFDF, TFDF viscous heating	(2)-(9)
[30] 2009	N	CWT H1	HDF, TDF, viscous dissipation, axial conduction	(6)-(11)

7. HEAT TRANSFER IN TRAPEZOIDAL OR TRIANGULAR MICROCHANNELS

Trapezoidal microchannels are also easily etched in silicon by chemical (for example with KOH) etching. The cross-section is defined by its depth h , its smallest width $2b$, and its side angle ϕ (see Fig. 1e). The aspect ratio of the section is $\alpha = h/(2b)$. Slip flow heat transfer in such channels has been investigated by Niazmand et al. [53] who considered a developing flow (HDF and TDF) with constant wall temperature. A control-volume based numerical method was employed, assuming first-order boundary conditions (2)-(9), $\Pr = 1$ and $\gamma = 1.4$. Different channel aspect ratios and side angles were investigated. Heat transfer is significantly reduced as Kn is increased in the entrance region. The following correlation was proposed for the fully developed Nusselt number:

$$Nu_{(\text{TR},\infty,\text{CWT})} = \left[2.87 \left(\frac{\pi}{2\phi} \right)^{-0.26} + 4.8 \exp\left(-3.9\alpha \left(\frac{\pi}{2\phi} \right)^{0.21} \right) \right] G_1 G_2 \quad (42)$$

with

$$G_1 = 1 - 1.75\, Kn^{0.64} \left(1 - 0.72 \tanh(2\alpha)\right) \quad (43)$$

and

$$G_2 = 1 + 0.075(1+\alpha)\exp\left(-0.45\, Re\, Pr\right). \quad (44)$$

This correlation is in agreement within 10% with the numerical simulations for all aspect ratios ($\alpha = \{0.25; 0.5; 1; 2\}$) and side angles ($\phi = \pi/n$ with $n = \{2; 3; 4; 6\}$) considered.

Kuddusi and Cetegen [54] considered the case of a microchannel etched by KOH in a silicon wafer, for which the crystalline structure of the substrate leads to an angle $\phi = 54.74°$. The constant heat flux problem H2-4 for thermally developing flow was numerically solved in a square computational domain obtained by transformation of the trapezoidal geometry. Numerical data on the Nusselt number were provided for different values of the aspect ratio.

Triangular microchannel is a specific case of trapezoidal microchannel, for which $\alpha = 0$. Slip flow heat transfer in isosceles triangular microchannels was investigated by Zhu et al. [55] who considered unsymmetrical heat conditions: one side insulated with two sides at constant temperature, or two sides insulated and one side at constant temperature. They finally proposed correlations for these two layouts in the case of an equilateral triangular section.

TABLE 5: SUMMARY OF INVESTIGATIONS ON SLIP FLOW HEAT TRANSFER IN TRAPEZOIDAL OR TRIANGULAR MICROCHANNELS.

Refs. Year	Kind of Work	Heat Conditions	Assumptions	BC
[53] 2008	N	CWT	HDF, TDF	(2)-(9)
[54] 2009	N	H2-4	HFDF, TDF	(3)-(10)
[55] 2004	AI	CWT-1WI CWT-2WI	HFDF, TFDF	(3)-(10)

8. HEAT TRANSFER IN MICROCHANNELS WITH OTHER SECTIONS

Microchannels with annular cross-sections

Slip-flow heat transfer with viscous dissipation in a micro-annulus, with uniform heat flux at one wall and adiabatic conditions at the other wall, was analytically studied by Avcı and Aydın [56]. The same geometry with constant wall temperature was numerically analyzed by Char and Tai [57], taking into account viscous dissipation.

Duan and Muzychka [58] published an explicit analytical solution for the fully developed Nusselt number in annular microchannels, considering either CHF at one wall and adiabatic conditions at the other wall, or CHF on both walls.

Microchannels with other kinds of cross-sections

Developments on slip flow heat transfer with CWT in microchannels with rhombus section can be found in [59], whereas considerations on the modeling of slip flow heat transfer in microchannels of arbitrary cross sections are presented in [60] and [61].

CONCLUSIONS

The literature on slip flow heat transfer is now well stocked, with a series of available analytical solutions or numerical analysis for various heat conditions and microchannel geometries. The limits of the analytical solutions, based on simplifying assumptions, are not, however, always well documented. The influence of variations in gas properties has been analyzed in details [62], but not yet in the slip flow regime.

On the other hand, although the theory of gas hydrodynamics in the slip flow regime is now supported by smart experiments [5, 40, 63], there is a crucial lack of experimental data concerning heat transfer in this regime. Providing accurate experimental data on slip flow heat transfer is a challenge for the next years, which would allow a real discussion on the validity of velocity slip and temperature jump boundary conditions, as well as on the limits of applicability of slip flow theory, in terms of degree of rarefaction.

ACKNOWLEDGMENTS

The support of the European Community under grant PITN-GA-2008-215504, ‘Gas flows in Micro Electro Mechanical Systems’ is gratefully acknowledged.

REFERENCES

1. Colin, S., *Rarefaction and compressibility effects on steady and transient gas flows in microchannels.* Microfluidics and Nanofluidics, 2005. **1**(3): p. 268-279.
2. Sobhan, C.B. and S.V. Garimella, *A comparative analysis of studies on heat transfer and fluid flow in microchannels.* Microscale Thermophysical Engineering, 2001. **5**(4): p. 293-311.
3. Rostami, A.A., A.S. Mujumdar, and N. Saniei, *Flow and heat transfer for gas flowing in microchannels: a review.* Heat and Mass Transfer, 2002. **38**(4-5): p. 359-367.
4. Morini, G.L., *Single-phase convective heat transfer in microchannels: a review of experimental results.*

International Journal of Thermal Sciences, 2004. **43**(7): p. 631-651.
5. Pitakarnnop, J., et al., *A novel experimental setup for gas microflows.* Microfluidics and Nanofluidics, 2010. **8**(1): p. 57-72.
6. Kandlikar, S.G., et al., *Heat transfer and fluid flow in minichannels and microchannels*. 2006, Oxford: Elsevier.
7. Sparrow, E.M. and S.H. Lin, *Laminar heat transfer in tubes under slip-flow conditions.* Journal of Heat Transfer, 1962. **84**: p. 363-369.
8. Ameel, T.A., et al., *Laminar forced convection in a circular tube with constant heat flux and slip flow.* Microscale Thermophysical Engineering, 1997. **1**(4): p. 303-320.
9. Li, J.-M., B.-X. Wang, and X.-F. Peng, *'Wall-adjacent layer' analysis for developed-flow laminar heat transfer of gases in microchannels.* International Journal of Heat and Mass Transfer, 2000. **43**(5): p. 839-847.
10. Tunc, G. and Y. Bayazitoglu, *Heat transfer in microtubes with viscous dissipation.* International Journal of Heat and Mass Transfer, 2001. **44**(13): p. 2395-2403.
11. Aydın, O. and M. Avcın, *Heat and fluid flow characteristics of gases in micropipes.* International Journal of Heat and Mass Transfer, 2006. **49**(9-10): p. 1723-1730.
12. Jeong, H. and J. Jeong, *Extended Graetz problem including axial conduction and viscous dissipation in microtube.* Journal of Mechanical Science and Technology, 2006. **20**(1): p. 158-166.
13. Hooman, K., *Entropy generation for microscale forced convection: Effects of different thermal boundary conditions, velocity slip, temperature jump, viscous dissipation, and duct geometry.* International Communications in Heat and Mass Transfer, 2007. **34**(8): p. 945-957.
14. Hooman, K. and A. Ejlali, *Effects of viscous heating, fluid property variation, velocity slip, and temperature jump on convection through parallel plate and circular microchannels.* International Communications in Heat and Mass Transfer, 2010. **37**(1): p. 34-38.
15. Hooman, K., F. Hooman, and M. Famouri, *Scaling effects for flow in micro-channels: Variable property, viscous heating, velocity slip, and temperature jump.* International Communications in Heat and Mass Transfer, 2009. **36**(2): p. 192-196.
16. Barron, R.F., et al., *Evaluation of the eigenvalues for the Graetz problem in slip-flow.* International Communications in Heat and Mass Transfer, 1996. **23**(4): p. 563-574.
17. Barron, R.F., et al., *The Graetz problem extended to slip-flow.* International Journal of Heat and Mass Transfer, 1997. **40**(8): p. 1817-1823.
18. Mikhailov, M.D. and R.M. Cotta, *Eigenvalues for the Graetz problem in slip flow.* International Communications in Heat and Mass Transfer, 1997. **24**(3): p. 449-451.
19. Larrodé, F.E., C. Housiadas, and Y. Drossinos, *Slip-flow heat transfer in circular tubes.* International Journal of Heat and Mass Transfer, 2000. **43**(15): p. 2669-2680.
20. Myong, R.S., D.A. Lockerby, and J.M. Reese, *The effect of gaseous slip on microscale heat transfer: An extended Graetz problem.* International Journal of Heat and Mass Transfer, 2006. **49**(15-16): p. 2502-2513.
21. Çetin, B., A.G. Yazicioglu, and S. Kakaç, *Slip-flow heat transfer in microtubes with axial conduction and viscous dissipation - An extended Graetz problem.* International Journal of Thermal Sciences, 2009. **48**(9): p. 1673-1678.
22. Çetin, B., A.G. Yazicioglu, and S. Kakaç, *Fluid flow in microtubes with axial conduction including rarefaction and viscous dissipation.* International Communications in Heat and Mass Transfer, 2008. **35**(5): p. 535-544.
23. Satapathy, A.K., *Slip flow heat transfer in an infinite microtube with axial conduction.* International Journal of Thermal Sciences, 2010. **49**(1): p. 153-160.
24. Demsis, A., et al., *Experimental determination of heat transfer coefficient in the slip regime and its anomalously low value.* Physical Review E, 2009. **80**(1): p. 016311.
25. Choi, S.B., R.F. Barron, and R.O. Warrington, *Fluid flow and heat transfer in microtubes*. 1991, ASME: New York. p. 123-133.
26. Inman, R., *Laminar slip flow heat transfer in a parallel plate channel or a round tube with uniform wall heating*, in *Technical Report NASA*. 1964.
27. Zhu, X., M.D. Xin, and Q. Liao, *Analysis of heat transfer between two unsymmetrically heated parallel plates with microspacing in the slip flow regime.* Microscale Thermophysical Engineering, 2002. **6**(4): p. 287-301.
28. Jeong, H.-E. and J.-T. Jeong, *Extended Graetz problem including streamwise conduction and viscous dissipation in microchannel.* International Journal of Heat and Mass Transfer, 2006. **49**(13-14): p. 2151-2157.
29. Aydın, O. and M. Avcı, *Analysis of laminar heat transfer in micro-Poiseuille flow.* International Journal of Thermal Sciences, 2007. **46**(1): p. 30-37.
30. van Rij, J., T. Ameel, and T. Harman, *The effect of viscous dissipation and rarefaction on rectangular microchannel convective heat transfer.* International Journal of Thermal Sciences, 2009. **48**(2): p. 271-281.
31. Hadjiconstantinou, N.G. and O. Simek, *Constant-wall-temperature Nusselt number in micro and nano-channels.* Journal of Heat Transfer, 2002. **124**: p. 356-364.
32. Kavehpour, H.P., M. Faghri, and Y. Asako, *Effects of compressibility and rarefaction on gaseous flows in microchannels*, in *Numerical Heat Transfer, Part A*. 1997. p. 677-696.
33. Yu, S. and T.A. Ameel, *Slip-flow Peclet number thermal entry problem within a flat microchannel subject to constant wall temperature*, in *Proceedings of the International Conference on Heat Transfer and Transport Phenomena in*

Microscale, G.P. Celata, Editor. 2000: Banff, Canada. p. 101-107.
34. Mikhailov, M.D. and R.M. Cotta, *Mixed symbolic-numerical computation of convective heat transfer with slip flow in microchannels.* International Communications in Heat and Mass Transfer, 2005. **32**(3-4): p. 341-348.
35. Khadem, M.H., M. Shams, and S. Hossainpour, *Numerical simulation of roughness effects on flow and heat transfer in microchannels at slip flow regime.* International Communications in Heat and Mass Transfer, 2009. **36**(1): p. 69-77.
36. Ji, Y., K. Yuan, and J.N. Chung, *Numerical simulation of wall roughness on gaseous flow and heat transfer in a microchannel.* International Journal of Heat and Mass Transfer, 2006. **49**(7-8): p. 1329-1339.
37. Croce, G. and P. D'Agaro, *Compressibility and rarefaction effect on heat transfer in rough microchannels.* International Journal of Thermal Sciences, 2009. **48**(2): p. 252-260.
38. Ebert, W.A. and E.M. Sparrow, *Slip flow in rectangular and annular ducts.* Journal of Basic Engineering, 1965. **87**: p. 1018-1024.
39. Aubert, C. and S. Colin, *High-order boundary conditions for gaseous flows in rectangular microchannels.* Microscale Thermophysical Engineering, 2001. **5**(1): p. 41-54.
40. Colin, S., P. Lalonde, and R. Caen, *Validation of a second-order slip flow model in rectangular microchannels.* Heat Transfer Engineering, 2004. **25**(3): p. 23-30.
41. Spiga, M. and G.L. Morini, *Nusselt numbers in laminar flow for H2 boundary conditions.* International Journal of Heat and Mass Transfer, 1996. **39**(6): p. 1165-1174.
42. Morini, G.L., *Analytical determination of the temperature distribution and Nusselt numbers in rectangular ducts with constant axial heat flux.* International Journal of Heat and Mass Transfer, 2000. **43**(5): p. 741-755.
43. Yu, S. and T.A. Ameel, *Slip-flow heat transfer in rectangular microchannels.* International Journal of Heat and Mass Transfer, 2001. **44**(22): p. 4225-4234.
44. Tunc, G. and Y. Bayazitoglu, *Heat transfer in rectangular microchannels.* International Journal of Heat and Mass Transfer, 2002. **45**(4): p. 765-773.
45. Yu, S. and T.A. Ameel, *Slip flow convection in isoflux rectangular microchannels.* Journal of Heat Transfer, 2002. **124**: p. 346-355.
46. Ghodoossi, L. and Egrican, *Prediction of heat transfer characteristics in rectangular microchannels for slip flow regime and H1 boundary condition.* International Journal of Thermal Sciences, 2005. **44**(6): p. 513-520.
47. Renksizbulut, M., H. Niazmand, and G. Tercan, *Slip-flow and heat transfer in rectangular microchannels with constant wall temperature.* International Journal of Thermal Sciences, 2006. **45**(9): p. 870-881.
48. Aynur, T., L. Kuddusi, and N. Eğrican, *Viscous dissipation effect on heat transfer characteristics of rectangular microchannels under slip flow regime and H1 boundary conditions.* Heat and Mass Transfer, 2006. **42**(12): p. 1093-1101.
49. Kuddusi, L. and E. Cetegen, *Prediction of temperature distribution and Nusselt number in rectangular microchannels at wall slip condition for all versions of constant heat flux.* International Journal of Heat and Fluid Flow, 2007. **28**(4): p. 777-786.
50. Hettiarachchi, H.D.M., et al., *Slip-flow and conjugate heat transfer in rectangular microchannels*, in *HT2008: Proceedings of the ASME Summer Heat Transfer Conference*. 2008. p. 547-555.
51. Hettiarachchi, H.D.M., et al., *Three-dimensional laminar slip-flow and heat transfer in a rectangular microchannel with constant wall temperature.* International Journal of Heat and Mass Transfer, 2008. **51**(21-22): p. 5088-5096.
52. Hooman, K., *Heat transfer and entropy generation for forced convection through a microduct of rectangular cross-section: Effects of velocity slip, temperature jump, and duct geometry.* International Communications in Heat and Mass Transfer, 2008. **35**(9): p. 1065-1068.
53. Niazmand, H., M. Renksizbulut, and E. Saeedi, *Developing slip-flow and heat transfer in trapezoidal microchannels.* International Journal of Heat and Mass Transfer, 2008. **51**(25-26): p. 6126-6135.
54. Kuddusi, L. and E. Çetegen, *Thermal and hydrodynamic analysis of gaseous flow in trapezoidal silicon microchannels.* International Journal of Thermal Sciences, 2009. **48**(2): p. 353-362.
55. Zhu, X., Q. Liao, and M. Xin, *Analysis of the heat transfer in unsymmetrically heated triangular microchannels in slip flow regime.* Science in China Series E: Technological Sciences, 2004. **47**(4): p. 436-446.
56. Avci, M. and O. Aydin, *Laminar forced convection slip-flow in a micro-annulus between two concentric cylinders.* International Journal of Heat and Mass Transfer, 2008. **51**(13-14): p. 3460-3467.
57. Char, M.-I. and B.-C. Tai, *Effects of viscous dissipation on slip-flow heat transfer in a micro annulus.* International Journal of Heat and Mass Transfer, 2010. **53**(7-8): p. 1402-1408.
58. Duan, Z. and Y.S. Muzychka, *Slip Flow Heat Transfer in Annular Microchannels With Constant Heat Flux.* Journal of Heat Transfer, 2008. **130**(9): p. 092401.
59. Shams, M., et al., *Numerical simulation of slip flow through rhombus microchannels.* International Communications in Heat and Mass Transfer, 2009. **36**(10): p. 1075-1081.
60. Zhu, X. and Q. Liao, *Heat transfer for laminar slip flow in a microchannel of arbitrary cross section with complex thermal boundary conditions.* Applied Thermal Engineering, 2006. **26**(11-12): p. 1246-1256.
61. Hooman, K., *A superposition approach to study slip-flow forced convection in straight microchannels of uniform but arbitrary cross-section.* International Journal of Heat and Mass Transfer, 2008. **51**(15-16): p. 3753-3762.

62. Gulhane, N.P. and S.P. Mahulikar, *Variations in gas properties in laminar micro-convection with entrance effect.* International Journal of Heat and Mass Transfer, 2009. **52**(7-8): p. 1980-1990.
63. Ewart, T., et al., *Mass flow rate measurements in gas micro flows.* Experiments in Fluids, 2006. **41**(3): p. 487-498.

